*International Journal of Toxicology*, 25:451–457, 2006

ISSN: 1091-5818 print / 1092-874X online
DOI: 10.1080/10915810600959543

# Toxicity of Cerium Oxide Nanoparticles in Human Lung Cancer Cells

**Weisheng Lin**
*Department of Chemistry and Environmental Research Center for Emerging Contaminants, University of Missouri-Rolla, Rolla, Missouri, USA*

**Yue-wern Huang**
*Department of Biological Sciences and Environmental Research Center for Emerging Contaminants, University of Missouri-Rolla, Rolla, Missouri, USA*

**Xiao-Dong Zhou**
*Pacific Northwest National Laboratory, Richland, Washington, USA*

**Yinfa Ma**
*Department of Chemistry and Environmental Research Center for Emerging Contaminants, University of Missouri-Rolla, Rolla, Missouri, USA*

**With the fast development of nanotechnology, the nanomaterials start to cause people's attention for potential toxic effect. In this paper, the cytotoxicity and oxidative stress caused by 20-nm cerium oxide ($CeO_2$) nanoparticles in cultured human lung cancer cells was investigated. The sulforhodamine B method was employed to assess cell viability after exposure to 3.5, 10.5, and 23.3 $\mu$g/ml of $CeO_2$ nanoparticles for 24, 48, and 72 h. Cell viability decreased significantly as a function of nanoparticle dose and exposure time. Indicators of oxidative stress and cytotoxicity, including total reactive oxygen species, glutathione, malondialdehyde, $\alpha$-tocopherol, and lactate dehydrogenase, were quantitatively assessed. It is concluded from the results that free radicals generated by exposure to 3.5 to 23.3 $\mu$g/ml $CeO_2$ nanoparticles produce significant oxidative stress in the cells, as reflected by reduced glutathione and $\alpha$-tocopherol levels; the toxic effects of $CeO_2$ nanoparticles are dose dependent and time dependent; elevated oxidative stress increases the production of malondialdehyde and lactate dehydrogenase, which are indicators of lipid peroxidation and cell membrane damage, respectively.**

**Keywords** Cerium Oxide ($CeO_2$), Cytotoxicity, Lung Cancer Cells (A549), Nanoparticles, Oxidative Stress

Nanomaterials are defined by the U.S. National Nanotechnology Initiative as materials that have at least one dimension in the 1- to 100-nm range. Due to their unique physical and chemical characteristics, nanoparticles have been the focus of many investigation and material applications of over the past 10 years (Mandal et al. 2006). As a lanthanide element oxide, cerium oxide ($CeO_2$) nanoparticles are one of the most important nanomaterials, finding use in a wide range of applications, including catalysis (Corma et al. 2004b; Zheng et al. 2005), solar cells (Corma et al. 2004a), fuel cells (Murray, Tsai, and Barnett 1999; Pati et al. 2004), phosphor/luminescence (Sato et al. 2004; Yu, Xie, and Su 2001), abrasives for chemical mechanical planarizations (Parker 2004; Feng et al. 2003), gas sensors, oxygen pumps, and metallurgical and glass/ceramic applications. These applications take advantage of cerium's high thermodynamic affinity for oxygen and sulfur, its potential redox chemistry involving Ce(III)/Ce(IV), and the unique useful absorption/excitation energy bands associated with its electronic structure.

Though the potential effects of nanoparticles on human health remain unclear, a few preliminary studies have demonstrated toxic effects of nano-scale particles (Bermudez et al. 2004; Dreher 2004; Hoet, Nemmar, and Nemery 2004; Tamura et al. 2004; Lam et al. 2004; Peters et al. 2004; Service 2004; Shvedova et al. 2003; Warheit 2004; Warheit et al. 2004). For instance, carbon nanomaterials (nanotubes and fullerene) (Kamat et al. 1998; Lam et al. 2004; Manna et al. 2005; Sayes et al. 2005), titanium dioxide (Gurr et al. 2005), quantum dots (Green and

Received 6 March 2006; accepted 21 June 2006.
The authors thank the Department of Chemistry, the Department of Biological Sciences, and the Environmental Research Center for Emerging Contaminants at the University of Missouri-Rolla for financial support, and appreciate Nuran Ercal and her students for their discussions and comments regarding GSH and MDA protocols. Thanks also go to Robert S. Aronstam for commenting on and editing the manuscript.
Address correspondence to Yinfa Ma, PhD, Professor of Chemistry, Department of Chemistry and Environmental Research Center for Emerging Contaminants, University of Missouri-Rolla, Rolla, MO 65409, USA. E-mail: yinfa@umr.edu

Howman 2005), ultrafine polystyrene (Brown et al. 2001), and ultrafine particulate pollutants (Feng et al. 2003) can interrupt cell function, causing cell membrane and DNA damage mainly through oxidative stress and lipid peroxidation. However, most of the nanoparticles that are commonly used in industries, including $CeO_2$, have not been systematically studied and their cytotoxicity potentials remain unknown.

In this study, we evaluated the cytotoxic effects of 20-nm $CeO_2$ nanoparticles using a human bronchoalveolar carcinoma-derived cell line (A549). Nanoparticles were dispersed in the cell culture medium at varying concentrations. Cytotoxicity was measured as cell viability using the sulforhodamine B (SRB) method (Skehan et al. 1990). The cytotoxicity of the nanoparticles as a function of exposure time was also investigated. To reveal possible mechanisms of cytotoxicity, some important biomarkers for oxidative stress and cytotoxicity, such as reactive oxygen species (ROS), glutathione (GSH), malondialdehyde (MDA), $\alpha$-tocopherol, and lactate dehydrogenase (LDH), were measured using high-performance liquid chromatography (HPLC) and other methods. The results indicated that the $CeO_2$ nanoparticles induce oxidative stress and cell membrane leakage.

## MATERIALS AND METHODS

### Nanoparticles

$CeO_2$ nanoparticles were synthesized with the room temperature homogeneous nucleation method (Zhou, Huebner, and Anderson 2003; Zhou, Anderson, and Huebner 2002). The size and distribution was $20 \pm 3$ nm. Transmission electron microscopy (TEM; Philips EM420) was used to characterize particle morphology, size, and agglomeration states. Particle size analysis was also carried out by measuring the specific surface area (SSA; $m^2/g$) of the powders through the Brunauer, Emmett, and Teller (BET) techniques (Quantachrome; Nova 1000). Corresponding x-ray diffractometry (XRD; Scintag 2000) was used to characterize particle crystallinity. TEM particle size, BET particle size, and XRD crystallite size were in good agreement, indicating a substantially low degree of particle agglomeration (Zhou, Huebner, and Anderson 2003; Zhou and Huebner 2001; Zhou, Anderson, and Huebner 2002).

Due to their nanoscale size and surface properties, nanoparticles tend to aggregate or precipitate in suspensions. Thus, we tested the homogeneity of nanoparticles in the A549 cell culture medium (Ham's F-12). Nanoparticle $CeO_2$ suspension was prepared in the cell culture medium and dispersed for 5 min by a sonicator (FS-60H, 130W, 20 kHz; Fisher Scientific, Pittsburg, PA, USA). Throughout the time period of the experiments, the $CeO_2$ suspension concentrations of 3.5, 10.5, and 23.3 $\mu$g/ml were stable and uniform in the cell culture medium. Higher concentrations were not used because the nanoparticles tended to aggregate and precipitate. Based on our previous broader-ranged dose-response studies, these doses were chosen because they resulted in gradually increasing levels of toxicity. In each study, the nanoparticle suspension was prepared fresh and immediately applied to the A549 cells.

### Chemicals

Fetal bovine serum was purchased from American Type Culture Collection (ATCC) (Manassas, VA, USA). Ham's F-12 medium with L-glutamine, HPLC-grade methanol, n-butanol, hexane, acetonitrile, and analytical grade 12 M hydrochloric acid were purchased from Fisher Scientific (Pittsburgh, PA, USA). Trypsin-EDTA ($1\times$) and Hank's balanced salt solution (HBSS) were purchased from Invitrogen (Carlsbad, CA, USA). Sulforhodamine B was bought from ICN Biomedicals (Irvine, CA, USA). Penicillin-streptomycin, trichloroacetic acid (TCA), 1,1,3,3-tetramethoxypropane, 2-thiobarbituric acid, ethanol (reagent grade), 2-vinylpyridine, *o*-phosphoric acid (HPLC grade), *N*-(1-pyrenyl)maleimide (NPM), 2′,7′-dichlorofluorescin diacetate, glutathione (reduced), $\alpha$-tocopherol, L-serine, boric acid, diethylenetriaminepentaacetic acid (DETAPAC), TRIS hydrochloride, butylated-hydroxytoluene (BHT), tetrahydrofuran, $Na_2HPO_4$, $NaH_2PO_4$, and acetic acid (HPLC grade) were obtained from Sigma-Aldrich (Saint Louis, MO, USA). Ultrapure deionized water was prepared using a Milli-Q system (Millipore, Bedford, MA, USA).

### Cell Culture and Treatment with $CeO_2$

The human bronchoalveolar carcinoma-derived cell line (A549) was purchased from ATCC (Manassas, VA, USA). The reason to choose this cell line is that it is a typical cancer line that has widely been used for in vitro cytotoxicity study (Huang, Khor, and Lim 2004). Cells were maintained in Ham's F-12 medium supplemented with 10% fetal bovine serum, 100 units/ml penicillin, and 100 $\mu$g/ml streptomycin, and grown at 37°C in a 5% $CO_2$ humidified environment. For the SRB assay and the determination of GSH, MDA, $\alpha$-tocopherol, and LDH levels, A549 cells were plated into 75-$cm^2$ flasks at a density of $2.0 \times 10^5$ cells per flask in 13 ml culture medium and allowed to attach for 48 h. Then, the freshly dispersed nanoparticle suspension in the cell culture medium was prepared and diluted to appropriate concentrations (3.5, 10.5, and 23.3 $\mu$g/ml) and then applied to the cells. Cells without $CeO_2$ treatment served as controls in each experiment.

After incubation with $CeO_2$ for an appropriate period of time, the cell culture medium was collected for LDH determination. The cells were rinsed with ice-cold phosphate-buffered saline (PBS) and trypsinized. Homogenates were prepared by freezing at −70°C until analyzed for levels of GSH, MDA, $\alpha$-tocopherol, and protein. For ROS determination, cells were plated at a density of $1.0 \times 10^5$ cells/well in a 24-well collagen-coated culture plate and allowed to attach for 48 h. The cells were then harvested, and total ROS was measured as described below.

### Assessment of Cytotoxicity

After the cells were exposed to $CeO_2$ nanoparticles for 24, 48, or 72 h, the experiments were terminated by removal of the medium, and the number of cells in each flask was determined using the SRB assay (Skehan et al. 1990). After discarding the medium, the cells were fixed with 10 ml cold 10% trichloroacetic acid (TCA). The TCA solution was then discarded, and the cells were washed three times with distillated water followed by drying under nitrogen. Five milliliter of 0.2% sulforhodamine B in a 1% acetic acid was added to each flask to stain the cells for 30 min. The staining solution was discarded and the cells were washed with 1% acetic acid to eliminate excess dye. After complete drying, the dye was dissolved in cold 10 mM Tris buffer (pH 10.5) of 5 ml per flask. One-hundred-microliter aliquots of dye solution in each flask were transferred into a 96-well plate and the absorbance was measured at 550 nm using a microplate reader (FLOURstar; BMG Labtechnologies, Durham, NC, USA).

### Intracellular ROS Measurement

The production of intracellular reactive oxygen species (ROS) was measured using 2′,7′-dichlorofluorescin diacetate (DCFH-DA) (Wang and Joseph 1999). DCFH-DA passively enters cell where it reacts with ROS to form the highly fluorescent compound dichlorofluorescein (DCF). Briefly, 10 mM DCFH-DA stock solution (in methanol) was diluted 500-fold in HBSS without serum or other additive to yield a 20 $\mu$M working solution of DCFH-DA. After 24 h exposure to $CeO_2$ nanoparticles, the cells in 24-well plate were washed twice with HBSS and then incubated in 2 ml working solution of DCFH-DA at 37°C for 30 min. Fluorescence was then read at 485-nm excitation and 520-nm emission using a microplate reader. Cell-free experiments with and without $CeO_2$ nanoparticles were also conducted to determine whether there was any possible generation of ROS by direct interaction of $CeO_2$ nanoparticles.

### LDH Measurement

Lactate dedydrogenase (LDH) activity in the cell medium was determined using an LDH Kit (Pointe Scientific, Lincoln Park, MI, USA). One hundred microliter of cell medium was used for LDH analysis. Absorption was measured using a Beckman DU-640B UV-Visible Spectrophotometer at 340 nm. This procedure is based on the method developed by Wacker et al. in 1956 (Wacker 1956), optimized for greater sensitivity and linearity. Released LDH catalyzed the oxidation of lactate to pyruvate with simultaneous reduction of $NAD^+$ to NADH. The rate of $NAD^+$ reduction was measured as an increase in absorbance at 340 nm. The rate of $NAD^+$ reduction was directly proportional to LDH activity in the cell medium.

### GSH Measurement

Cellular levels of GSH were determined using the method described by Winters et al. (1995). After freezing at −70°C, the cells were homogenized in serine borate buffer (100 mM Tris-HCl, 10 mM boric acid, 5 mM L-serine, 1 mM DETAPAC, pH 7.5). Twenty microliter of homogenate was added to 230 $\mu$l HPLC grade $H_2O$ and 750 $\mu$l NMP solution (1 mM in acetonitrile). The resulting suspensions were incubated for 5 min at room temperature, then 5 $\mu$l of 2 N HCl was added to stop the reaction. The samples were filtered through a 0.2-$\mu$m Whatman Puradisc syringe filter, and an aliquot of 20 $\mu$l was injected for analysis using a Perkin-Elmer HPLC system with fluorescence detection (excitation at 330 nm, emission at 375 nm) and a 5-$\mu$m Reliasil C18 column (250 × 4.6 mm). The mobile phase consisted of 70% acetonitrile, 30% HPLC $H_2O$ containing 1 ml/L acetic acid, and 1 ml/L *o*-phosphoric acid. The flow rate was 1.0 ml/min.

### MDA Measurement

The concentration of malondialdehyde (MDA) was determined by the method describe by Draper et al. (1993) with some modifications. An aliquot 350 $\mu$l of cell homogenate was mixed with 100 $\mu$l of 500 ppm BHT (dissolved in methanol) and 550 $\mu$l of 10% TCA. The resulting mixture was boiled for 30 min to precipitate the proteins. After cooling on ice, the sample was centrifuged at 1,500 × *g* for 10 min. The supernatant was collected and 500 $\mu$l was mixed with 500 $\mu$l of a saturated aqueous TBA solution. This mixture was heated in a boiling water bath for 30 min. After cooling to room temperature, 500-$\mu$l samples were extracted with 1 ml of n-butanol using a Vortex mixer and then centrifuged at 1000 × *g* for 5 min. The top layer was collected and filtered through a 0.2-$\mu$m Whatman Puradisc syringe filter followed by analysis with the same Perkin-Elmer HPLC system and column as for GSH. Excitation wavelength and excitation wavelength were set at 515 nm and 550 nm, respectively. Twenty microliter samples were injected for analysis. The mobile phase consisted of 69.4% 5 mM sodium phosphate buffer (pH 7.0), 30% acetonitrile, and 0.6% THF. The flow rate of mobile phase was 1.0 ml/min.

### $\alpha$-Tocopherol Measurement

The method to extract cellular $\alpha$-tocopherol was described by Lang, Gohil, and Packer (1986). These procedures were exactly followed, and the extracted sample solution was filtered before HPLC analysis performed using the same Perkin-Elmer HPLC system and column as for GSH analysis. The excitation wavelength was 292 nm whereas emission wavelength was 324 nm. Twenty-microliter samples were injected for analysis. The mobile phase was 100% methanol and the flow rate was 1 ml/min.

### Protein Assay

The total protein concentration was measured by the Bradford method (Bradford 1976) using a BioRad Assay Kit (BioRad, Richmond, CA). Bovine serum albumin was used as a standard.

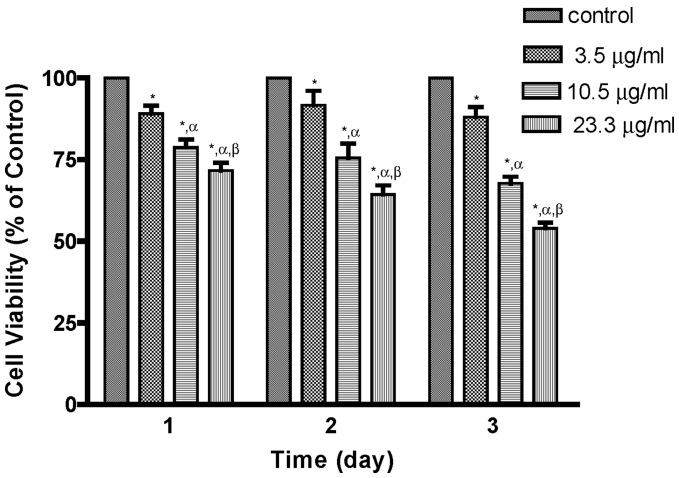


**FIGURE 1**
Viability of A549 cells after 24, 48, and 72 h exposure to 3.5, 10.5, or 23.3 $\mu$g/ml of 20 nm $CeO_2$. Values are mean $\pm$ *SD* ($n = 3$). Significance indicated by $^{*}p < .05$ versus control cells; $^{\alpha}p < .05$ versus cells exposed to 3.5 $\mu$g/ml $CeO_2$; $^{\beta}p < .05$ versus cells exposed to 10.5 $\mu$g/ml $CeO_2$.

### Statistics

Data were expressed as the mean $\pm$ *SD* of three experiments. One-tailed unpaired Student's $t$ test was used for significance testing, using a $p$ value of .05.

## RESULTS

### A549 Cell Viability and Cytotoxicity

A549 cells were exposed to $CeO_2$ at 3.5, 10.5, and 23.3 $\mu$g/ml for 24, 48, or 72 h. Cell viability decreased as a function of nanoparticle concentration (Figure 1). After 72 h of exposure to 3.5, 10.5, and 23.3 $\mu$g/ml of 20-nm $CeO_2$ nanoparticles, cell viability decreased to 88.0%, 67.7%, and 53.9%, respectively.

The extent of cell membrane breakage of A549 cells was revealed by LDH levels in cell medium. The LDH levels in the cell culture were increased in all treatment groups after exposure to $CeO_2$ nanoparticles for a period of 72 h ($p < .05$; Figure 2). LDH increased by 14.5%, 32.1%, and 70.5%, respectively. The LDH levels at the 23.3 $\mu$g/ml group were significantly greater than all other groups.

### Oxidative Stress Level in A549 Cells

DCF fluorescence intensity, indicative of oxidative stress (OS) levels in the cells, increased after 24 h of exposure to all concentration. DCF fluorescence intensity increased by 70%, 139%, and 181% after exposure to 3.5, 10.5, and 23.3 $\mu$g/ml, respectively, compared to the controls (Figure 3). The results showed a dose-dependent increase in fluorescence compared to control cells thereby indicating generation of ROS by $CeO_2$ nanoparticles in A549 cells. This oxidative stress to cells could cause the decrease of cell proliferation or even cell death via an apoptotic or necrosis pathway (Higuchi 2004). The results

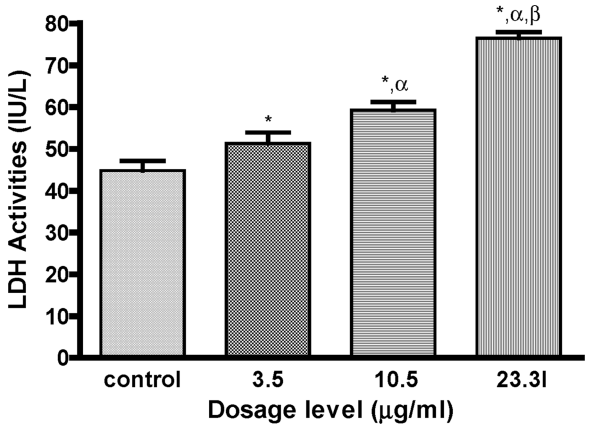


**FIGURE 2**
The LDH activities in the cell culture medium after 72 h exposure to 3.5, 10.5, or 23.3 $\mu$g/ml of 20 nm $CeO_2$. Values are mean $\pm$ *SD* ($n = 3$). The $p$ value indications were the same as those of Figure 1.

from cell-free positive-control experiments demonstrated that there was no ROS generation by direct interaction of 20-nm $CeO_2$ nanoparticles, which means that the OS levels were from the cells after exposure to 20-nm $CeO_2$ nanoparticles, not the 20-nm $CeO_2$ nanoparticles themselves (data were not shown).

### Antioxidant Levels in A549 Cells

The patterns of the cellular GSH levels agree with the dose-dependent response observed in the cell viability study (Figure 4). The maximum decrease after a 72-h exposure to 20-nm $CeO_2$ of cellular GSH levels ranged between 32.0% and 47.8%, respectively. There is a recovery of GSH level after 72 h of exposure; the lowest levels of GSH were observed after 48 h with each concentration. A dose-dependent reduction of $\alpha$-tocopherol was observed after the cells were exposed to $CeO_2$

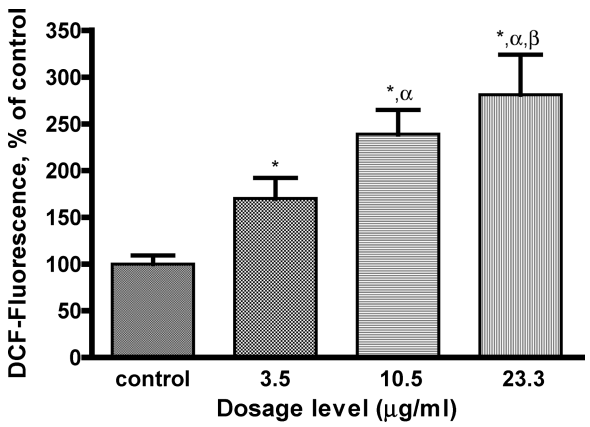


**FIGURE 3**
The relative levels of intracellular reactive oxygen species (ROS) after 24 h exposure to 3.5, 10.5, or 23.3 $\mu$g/ml of 20 nm $CeO_2$, indicated by DCF-fluorescence intensity. Values are mean $\pm$ *SD* ($n = 3$). The actual fluorescence value from those of the control cells was 1690 $\pm$ 155. The $p$ value indications were the same as those of Figure 1.

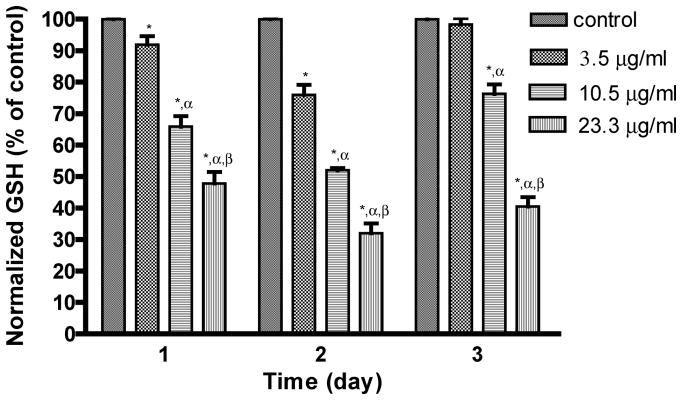


**FIGURE 4**
Normalized cellular GSH levels of A-549 cells after 24, 48, or 72 h exposure to 3.5, 10.5, or 23.3 $\mu$g/ml of 20 nm $CeO_2$. Values are mean $\pm$ *SD* ($n$ =3). The $p$ value indications were the same as those of Figure 1.

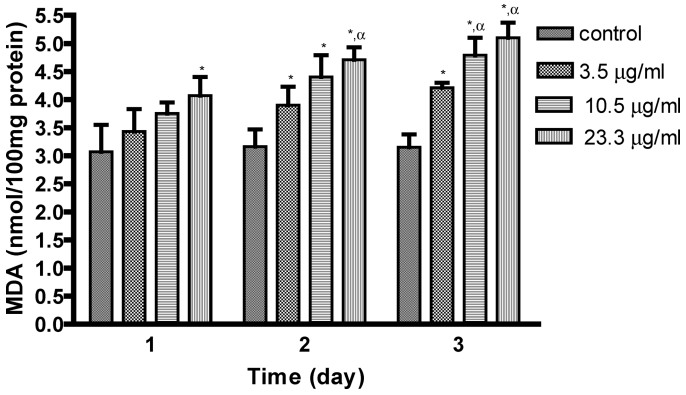


**FIGURE 6**
Cellular MDA levels of A-549 cells after 24, 48, or 72 h exposure to 3.5, 10.5, or 23.3 $\mu$g/ml of 20 nm $CeO_2$. Values are mean $\pm$ *SD* ($n$ =3). The $p$ value indications were the same as those of Figure 1.

for 72 h (Figure 5). $\alpha$-Tocopherol levels at exposure levels of 3.5, 10.5, and 23.3 $\mu$g/ml of $CeO_2$ decreased by 38.1%, 75.6%, and 87.5%, respectively, compared to untreated cells. The $\alpha$-tocopherol level at the 23.3 $\mu$g/ml after 72 h of exposure was significantly lower than those in the other groups, with only 13% of the cells complement of $\alpha$-tocopherol remaining (Figure 5).

### Lipid Peroxidation in A549 Cells

After being exposed to $CeO_2$ for 24 h, cellular MDA levels showed an increase with only the highest (23.3 $\mu$g/ml) $CeO_2$ dosage level (Figure 6). The MDA levels were significantly increased at cell concentration levels after a 48-h exposure. MDA levels were further increased after 72 h of exposure. Compared to the control groups, MDA levels increased by 23.4%, 39.2%, and 49.1% after 48 h of exposure at the dosage levels of 3.5, 10.5, and 23.3 $\mu$g/ml of $CeO_2$, respectively, whereas the corresponding increases after 72 h of exposure were 33.7%, 52.1%, and 61.9%, respectively.

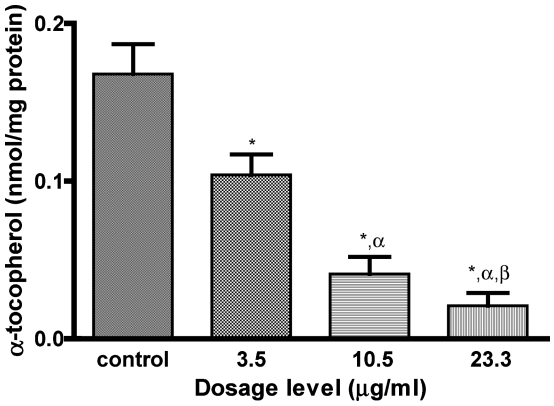


**FIGURE 5**
Cellular $\alpha$-tocopherol levels of A549 cells after 72 h exposure to 3.5, 10.5, or 23.3 $\mu$g/ml of 20 nm $CeO_2$. Values are mean $\pm$ *SD* ($n$ =3). The $p$ value indications were the same as those of Figure 1.

## DISCUSSION

We investigated the toxicity of 20-nm $CeO_2$ nanoparticles in A549 cells. The results demonstrated that 20-nm $CeO_2$ nanoparticles at dosage levels of 3.5 to 23.3 $\mu$g/ml can induce significant oxidative stress, as revealed by elevated ROS levels, reduced GSH levels, increased lipid peroxidation, and increased membrane damage. There is a strong correlation between decreased cell viability and the increased OS level after 24 h of exposure ($R^2 = .98$). A significant correlation was also observed between the decreased cell viability and increased LDH activity ($R^2 = .93$), indicating that cell death is the primary cause of the cell number reduction. Together, these results indicate that the reduction of cell viability is due to increased cellular stress that results in increased cell mortality, as indicated by elevated LDH activity. It is worth to mention that even though both assays can measure cell viability, but the LDH assay provides additional information about cell membrane damage. Because the final number of live cells is determined by the level of cell death and the rate of cell division, the LDH assay indicates the level of cell death.

The elevated oxidative stress is reflected in the reduced GSH and $\alpha$-tocopherol content, two crucial antioxidants (Figures 4 and 5). There is a linear relationship between the oxidative stress level represented by the DCF fluorescence and the $\alpha$-tocopherol level ($R^2 = .99$), whereas the relationship between the oxidative stress level and the GSH content is nonlinear. Additionally, there is a recovery of GSH levels after 72 h of exposure (Figure 4). A possible reason for this phenomenon is the recycling of oxidized GSH (GSSG) by the cell defense system via a coupled reaction involving GSH reductase and glucose-6-phosphate dehydrogen (G-6-PDH) (Nordberg and Arner 2001). The detailed molecular and biochemical mechanism underlying the GSH recovery warrants further research. The ratio of GSSG and GSH has often been used as an indicator of the levels of cellular oxidative stress. In addition to measuring GSH levels, we also attempted to detect GSSG levels in the cells. We were able to

detect the levels of spiked GSSG, but the levels of GSSG in the A549 cell samples were always below the detection limit. In theory, GSSG should be detectable because two GSH are converted to one GSSG during oxidation. However, binding of GSSG to cellular proteins may make it undetectable (Camera and Picardo 2002). In summary, free radical species generated by exposure to $CeO_2$ significantly reduces cellular antioxidant levels. Similar observations have been obtained by other researchers studying cellular oxidative stress and antioxidant levels after exposure to nanoparticles (Gurr et al. 2005; Green and Howman 2005; Shvedova et al. 2003; Tamura et al. 2004). However, a systematic study of $CeO_2$ nanoparticles has not been reported.

One of the consequences of elevated oxidative stress is the production of malondialdehyde, an indicator of lipid peroxidation (Figure 6). Lipid peroxidation caused by exposure to nanosize particles has been observed in other studies of nanoparticle toxicity (Draper et al. 1993; Gurr et al. 2005). Our data are the first to indicate cellular damage resulting from elevated oxidative stress by exposure to $CeO_2$ nanoparticles.

The mechanism of oxidative stress induced by nanoparticles is not well understood. However, there is evidence that free radicals can be induced at the surface of nanoparticles such as single-wall carbon nanotube (SWCNT) (Shvedova et al. 2003), semiconductor quantum dots (Green and Howman 2005), $TiO_2$ (Gurr et al. 2005), environmental particles (e.g., PM-10), asbestos, and a range of man-made fibers (Donaldson, Beswick, and Gilmour 1996). Based on the results of cytotoxicity of SWCNT (Shvedova et al. 2003) and potential redox property of $CeO_2$ nanoparticles involving Ce(III)/Ce(IV) (Flytzani-Stephanopoulos 2001), we propose the following sequential chemical reactions. Reactive species such as hydrogen peroxide ($H_2O_2$) and hydroxyl radical ($OH^{\cdot}$) are generated by reactions 1, 2, 3, and 4 below. Additionally, alkoxyl radicals from lipid peroxide (LOOH) may also be produced (reaction 5). In reaction 1, $A^-_{red}$ refer to physiologically relevant reductants, such as ascorbate and thiol compounds, whereas $A_{ox}$ are their oxidized states. The generated reactive oxygen species may cause oxidative stress and lipid peroxidation of A549 cells.

$$Ce^{4+} + A^-_{red} \longrightarrow Ce^{3+} + A_{ox} \quad [1]$$

$$Ce^{3+} + O_2 \longrightarrow Ce^{4+} + O_2^- \quad [2]$$

$$O_2^- + O_2^- + 2H^+ \longrightarrow O_2 + H_2O_2 \quad [3]$$

$$H_2O_2 + Ce^{3+} \longrightarrow Ce^{4+} + OH^- + OH^{\cdot} \quad [4]$$

$$LOOH + Ce^{3+} \longrightarrow Ce^{4+} + LO^{\cdot} + OH^- \quad [5]$$

In this study, we only studied $CeO_2$ of 20-nm size. A previous study using titanium of diameters 3, 10, 50, and 150 $\mu$m and titanium oxides of diameters 3, 50, and 500 nm showed that the survival rate of neutrophils decreased as the particle size decreased (Tamura et al. 2004). Size-dependent effects have also been observed in other studies with micro- to nano-size particles (Gurr et al. 2005; Peters et al. 2004; Donaldson, Beswick, and Gilmour 1996). Size-dependent toxicity of $CeO_2$ nanoparticles warrants further investigation. Furthermore, other chemical and physical parameters, such as composition, shape, surface activities, surface treatment, crystallinity, and agglomeration state, are also likely to affect the cytotoxicity of $CeO_2$ nanoparticles (Warheit, Webb, and Reed 2006; Warheit et al. 2006; Warheit et al. 2005). These properties will be further studied.

The expression of a wide variety of genes is sensitive to reactive active-oxygen species at the transcriptional level. Among the genes known to be activated by oxidative stress are those for mitogen-activated protein (MAP) kinase signaling, DNA damage, cyclic adenosine monophosphate (cAMP)/$Ca^{2+}$ signaling, nuclear factor kappa B (NF$\kappa$B) signaling, PI3-AKT (phosphoinositide 3-kinase/Akt) signaling, and apoptosis (Kharasch et al. 2005; Foncea et al. 2000). We are currently studying the expression of genes in these signaling pathways in response to exposure to $CeO_2$ (Desikan et al. 2001; Gasch et al. 2000; Demple 1991).

In conclusion, we have demonstrated that (1) 20-nm $CeO_2$ nanoparticles reduce cell viability in human bronchoalveolar carcinoma-derived cells; (2) free radicals generated by exposure to $CeO_2$ nanoparticles of 3.5 to 23.3 $\mu$g/ml produce significant oxidative stress in the cells, as reflected by reduced GSH and $\alpha$-tocopherol levels; (3) the toxic effects of 20-nm $CeO_2$ nanoparticles are both dose and time dependent; and (4) elevated oxidative stress increases the production of MDA and LDH, indicators of lipid peroxidation and membrane damage, respectively.

## REFERENCES


Bermudez, E., J. B. Mangum, B. A. Wong, B. Asgharian, P. M. Hext, D. B. Warheit, and J. I. Everitt. 2004. Pulmonary responses of mice, rats, and hamsters to subchronic inhalation of ultrafine titanium dioxide particles. *Toxicol. Sci.* 77:347–357.

Bradford, M. M. 1976. A rapid and sensitive method for the quantitation of microgram quantities of protein utilizing the principle of protein-dye binding. *Anal. Biochem.* 72:248–254.

Brown, D. M., M. R. Wilson, W. MacNee, V. Stone, and K. Donaldson. 2001. Size-dependent proinflammatory effects of ultrafine polystyrene particles: A role for surface area and oxidative stress in the enhanced activity of ultrafines. *Toxicol. Appl. Pharmacol.* 175:191–199.

Camera, E., and M. Picardo. 2002. Analytical methods to investigate glutathione and related compounds in biological and pathological processes. *J. Chromatogr. B Analyt. Technol. Biomed. Life Sci.* 781:181–206.

Corma, A., P. Atienzar, H. Garcia, and J. Y. Chane-Ching. 2004a. Hierarchically mesostructured doped $CeO_2$ with potential for solar-cell use. *Nat. Mater.* 3:394–397.

Corma, A., J. Y. Chane-Ching, M. Airiau, and C. Martinez. 2004b. Synthesis and catalytic properties of thermally and hydrothermally stable, high-surface-area $SiO_2$-$CeO_2$ mesostructured composite materials and their application for the removal of sulfur compounds from gasoline. *J. Catalysis* 224:441–448.

Demple, B. 1991. Regulation of bacterial oxidative stress genes. *Annu. Rev. Genet.* 25:315–337.

Desikan, R., A. H-Mackerness S, J. T. Hancock, and S. J. Neill. 2001. Regulation of the Arabidopsis transcriptome by oxidative stress. *Plant Physiol.* 127:159–172.

Donaldson, K., P. H. Beswick, and P. S. Gilmour. 1996. Free radical activity associated with the surface of particles: A unifying factor in determining biological activity? *Toxicol. Lett.* 88:293–298.

Draper, H. H., E. J. Squires, H. Mahmoodi, J. Wu, S. Agarwal, and M. Hadley. 1993. A comparative evaluation of thiobarbituric acid methods for the determination of malondialdehyde in biological materials. *Free Radic. Biol. Med.* 15:353–363.

Dreher, K. L. 2004. Health and environmental impact of nanotechnology: Toxicological assessment of manufactured nanoparticles. *Toxicol. Sci.* 77: 3–5.

Feng, X., Y.-S. Her, W. L. Zhang, J. Davis, E. Oswald, J. Lu, V. Bryg, S. Freeman, and D. Gnizak. 2003. $CeO_2$ particles for chemical mechanical planarization. *Mater. Res. Soc. Symp. Proc.* 767:173–183.

Flytzani-Stephanopoulos, M. 2001. Nanostructured cerium oxide "Ecocatalysts." *MRS Bulle.* 26:885–889.

Foncea, R., C. Carvajal, C. Almarza, and F. Leighton. 2000. Endothelial cell oxidative stress and signal transduction. *Biol. Res.* 33:89–96.

Gasch, A. P., P. T. Spellman, C. M. Kao, O. Carmel-Harel, M. B. Eisen, G. Storz, D. Botstein, and P. O. Brown. 2000. Genomic expression programs in the response of yeast cells to environmental changes. *Mol. Biol. Cell* 11:4241–4257.

Green, M., and E. Howman. 2005. Semiconductor quantum dots and free radical induced DNA nicking. *Chem. Commun. (Camb.)* 7:121–123.

Gurr, J. R., A. S. Wang, C. H. Chen, and K. Y. Jan. 2005. Ultrafine titanium dioxide particles in the absence of photoactivation can induce oxidative damage to human bronchial epithelial cells. *Toxicology* 213:66–73.

Higuchi, Y. 2004. Glutathione depletion-induced chromosomal DNA fragmentation associated with apoptosis and necrosis. *J. Cell. Mol. Med.* 8:455–464.

Hoet, P. H., A. Nemmar, and B. Nemery. 2004. Health impact of nanomaterials? *Nat. Biotechnol.* 22:19.

Huang, M., E. Khor, and L. Y. Lim. 2004. Uptake and cytotoxicity of chitosan molecules and nanoparticles: Effects of molecular weight and degree of deacetylation. *Pharm. Res.* 21:344–353.

Kamat, J. P., T. P. Devasagayam, K. I. Priyadarsini, H. Mohan, and J. P. Mittal. 1998. Oxidative damage induced by the fullerene C60 on photosensitization in rat liver microsomes. *Chem. Biol. Interact.* 114:145–159.

Kharasch, E. D., J. L. Schroeder, T. Bammler, R. Beyer, and S. Srinouanprachanh. 2005. Gene expression profiling of nephrotoxicity from the sevoflurane degradation product fluoromethyl-2,2-difluoro-1-(trifluoromethyl)vinyl ether ("compound A") in rats. *Toxicol. Sci.* 29:29.

Lam, C. W., J. T. James, R. McCluskey, and R. L. Hunter. 2004. Pulmonary toxicity of single-wall carbon nanotubes in mice 7 and 90 days after intratracheal instillation. *Toxicol. Sci.* 77:126–134.

Lang, J. K., K. Gohil, and L. Packer. 1986. Simultaneous determination of tocopherols, ubiquinols, and ubiquinones in blood, plasma, tissue homogenates, and subcellular fractions. *Anal. Biochem.* 157:106–116.

Mandal, D., M. E. Bolander, D. Mukhopadhyay, G. Sarkar, and P. Mukherjee. 2006. The use of microorganisms for the formation of metal nanoparticles and their application. *Appl. Microbiol. Biotechnol.* 69:485–492.

Manna, S. K., S. Sarkar, J. Barr, K. Wise, E. V. Barrera, O. Jejelowo, A. C. Rice-Ficht, and G. T. Ramesh. 2005. Single-walled carbon nanotube induces oxidative stress and activates nuclear transcription factor-kappaB in human keratinocytes. *Nano. Lett.* 5:1676–1684.

Murray, E. P., T. Tsai, and S. A. Barnett. 1999. A direct methane fuel cell with a ceria based a node. *Nature* 400:649–651.

Nordberg, J., and E. S. Arner. 2001. Reactive oxygen species, antioxidants, and the mammalian thioredoxin system. *Free. Radic. Biol. Med.* 31:1287–1312.

Parker, J. 2004. Next-generation abrasive particles for CMP. *Solid State Technol.* 47:30–32.

Pati, R. K., I. C. Lee, D. Chu, S. Hou, and S. H. Ehrman. 2004. Nanosized ceria based water-gas shift (WGS) catalyst for fuel cell applications. *Am. Chem. Soc., Div. Fuel Chem.* 49:953.

Peters, K., R. E. Unger, C. J. Kirkpatrick, A. M. Gatti, and E. Monari. 2004. Effects of nano-scaled particles on endothelial cell function in vitro: Studies on viability, proliferation and inflammation. *J. Mater. Sci. Mater. Med.* 15:321–325.

Sato, T., T. Katakura, S. Yin, T. Fujimoto, and S. Yabe. 2004. Synthesis and UV-shielding properties of calcia-doped ceria nanoparticles coated with amorphous silica. *Solid State Ionics* 172:377–382.

Sayes, C. M., A. M. Gobin, K. D. Ausman, J. Mendez, J. L. West, and V. L. Colvin. 2005. Nano-C60 cytotoxicity is due to lipid peroxidation. *Biomaterials* 26:7587–7595.

Service, R. F. 2004. Nanotoxicology. Nanotechnology grows up. *Science* 304:1732–1734.

Shvedova, A. A., V. Castranova, E. R. Kisin, D. Schwegler-Berry, A. R. Murray, V. Z. Gandelsman, A. Maynard, and P. Baron. 2003. Exposure to carbon nanotube material: assessment of nanotube cytotoxicity using human keratinocyte cells. *J. Toxicol. Environ. Health A* 66:1909–1926.

Skehan, P., R. Storeng, D. Scudiero, A. Monks, J. McMahon, D. Vistica, J. T. Warren, H. Bokesch, S. Kenney, and M. R. Boyd. 1990. New colorimetric cytotoxicity assay for anticancer-drug screening. *J. Natl. Cancer Inst.* 82:1107–1112.

Tamura, K., N. Takashi, T. Akasaka, I. D. Roska, M. Uo, Y. Totsuka, and F. Watari. 2004. Effects of micro/nano particles size on cell function and morphology. *Key Engin. Mater.* 254–256:919–922.

Wacker, W. E. C., et al. 1956. Metalloenzymes and myocardial infarction. II. Malic and lactic dehydrogenase activities and cinc concentrations in serum. *N. Engl. J. Med.* 255:449.

Wang, H., and J. A. Joseph. 1999. Quantifying cellular oxidative stress by dichlorofluorescein assay using microplate reader. *Free. Radic. Biol. Med.* 27:612–616.

Warheit, D. B. 2004. Nanoparticles: Health impacts? *Mater. Today* 7:32–35.

Warheit, D. B., W. J. Brock, K. P. Lee, T. R. Webb, and K. L. Reed. 2005. Comparative pulmonary toxicity inhalation and instillation studies with different $TiO_2$ particle formulations: Impact of surface treatments on particle toxicity. *Toxicol. Sci.* 88:514–524.

Warheit, D. B., B. R. Laurence, K. L. Reed, D. H. Roach, G. A. Reynolds, and T. R. Webb. 2004. Comparative pulmonary toxicity assessment of single-wall carbon nanotubes in rats. *Toxicol. Sci.* 77:117–125.

Warheit, D. B., K. L. Reed, J. D. Stonehuerner, A. J. Ghio, and T. R. Webb. 2006. Biodegradability of para-aramid respirable-sized fiber-shaped particulates (RFP) in human lung cells. *Toxicol. Sci.* 89:296–303.

Warheit, D. B., T. R. Webb, and K. L. Reed. 2006. Pulmonary toxicity screening studies in male rats with $TiO_2$ particulates. *Part Fibre Toxicol.* 3:3.

Winters, R. A., J. Zukowski, N. Ercal, R. H. Matthews, and D. R. Spitz. 1995. Analysis of glutathione, glutathione disulfide, cysteine, homocysteine, and other biological thiols by high-performance liquid chromatography following derivatization by n-(1-pyrenyl)maleimide. *Anal. Biochem.* 227:14–21.

Yu, X., P. Xie, and Q. Su. 2001. Size-dependent optical properties of nanocrystalline $CeO_2$: Er obtained by combustion synthesis. *Phys. Chem. Chem. Phys.* 3:5266–5269.

Zheng, X., X. Zhang, X. Wang, S. Wang, and S. Wu. 2005. Preparation and characterization of $CuO/CeO_2$ catalysts and their applications in low-temperature CO oxidation. *Appl. Catal. A Gen.* 295:142–149.

Zhou, X.-D., H. U. Anderson, and W. Huebner. 2002. Room temperature homogenous nucleation synthesis and thermal stability of nanometer $CeO_2$ single crystals. *Appl. Phys. Lett.* 80:3184–3186.

Zhou, X.-D., and W. Huebner. 2001. Size-induced lattice relaxation in $CeO_2$ nanoparticles. *Appl. Phys. Lett.* 79:3512–3514.

Zhou, X.-D., W. Huebner, and H. U. Anderson. 2003. Processing of nanometer-scale $CeO_2$ particles. *Chem. Mater.* 15:378–382.